Research Article | Vol. 26, No. 26 | 24 Dec 2018 | OPTICS EXPRESS 34655
Optics EXPRESS

Hot water-assisted fabrication of chirped polymer optical fiber Bragg gratings

RUI MIN,[1,*] BEATRIZ ORTEGA,[1] CHRISTIAN BROADWAY,[2] CHRISTOPHE CAUCHETEUR,[2] GETINET WOYESSA,[3] OLE BANG,[3,4] PAULO ANTUNES,[5] AND CARLOS MARQUES[5]

[1]*ITEAM Research Institute, Universitat Politècnica de València 46022 Valencia, Spain*
[2]*Electromagnetism and Telecommunication Department, University of Mons 7000 Mons, Belgium*
[3]*DTU Fotonik, Department of Photonics Engineering, Technical University of Denmark, Denmark*
[4]*SHUTE Sensing Solutions A/S, Oldenvej 1A 3490 Kvistgård, Denmark*
[5]*Instituto de Telecomunicações and Physics Department & I3N, Universidade de Aveiro, Portugal*
**rumi@doctor.upv.es*

Abstract: We obtained chirped gratings by performing hot water gradient thermal annealing of uniform poly (methylmethacrylate) (PMMA) microstructured polymer optical fiber Bragg gratings (POFBGs). The proposed method's simplicity is one of its main advantages because no special phase mask or additional etching are needed. It not only enables easy control tuning of the central wavelength and chirp characteristics, but it also leads to obtain flexible grating response, compared with tapered chirped POFBGs. Therefore, a flexible and low-cost chirped POFBG devices fabrication technique has been presented by using a single uniform phase mask.

1. Introduction

Polymer optical fibers (POFs) bring new opportunities for fiber Bragg grating (FBG) devices due to a lower Young's modulus and a larger range of applying strain [1]. Furthermore, POFs are ideal candidates for bio-sensing applications [2–5] due to their flexibility in bending, biocompatibility and non-brittle nature. Since the first polymer optical fiber Bragg grating (POFBG) was reported in 1999 [6], different polymer materials are used for FBG fabrication with specific purposes, such as low attenuation CYTOP [7], high temperature resistance and humidity insensitive Zeonex [8], polycarbonate [9], TOPAS [10], and mixtures thereof [11]. However, poly (methyl methacrylate) (PMMA) is the most common material for Bragg grating devices [1,6].

POFBGs are usually obtained using the phase mask technology, which is a simple and reliable method. However, the phase mask can only inscribe gratings with a given period, i.e., with a specific Bragg wavelength, whereas a Bragg grating centered at a different wavelength requires a new phase mask with another pitch value or using additional techniques, such as post-annealing [12], shown to provide a 230 nm tuning range [13], or straining the POF during FBG writing, shown to provide a 12 nm tuning range [14]. At the same time, non-uniform devices, such as chirped FBGs (CFBG) are attractive for other applications, such as dispersion compensation [15] and biomedical sensing [16], where POF materials show huge advantages compared with silica fibers, such as a lower Young's modulus, higher sensitivities, and biocompatibility and biodegradability [17]. In 2005, CFBGs in POF were proposed for the first time by *Liu et al* [18] based on taper technology. Recently, the first CFBG in POF was fabricated by using chirped phase mask technology [19], whereas tunable POF CFBGs have been obtained using taper technology [20] for a variety of applications, such as bio-medical thermal detection [21] or variable delay lines [22]. The use of a chirped phase mask is expensive and not flexible, whereas taper technology needs accurate tapering process and chirp characteristic changes with strain.

#349629 https://doi.org/10.1364/OE.26.034655
Journal © 2018 Received 31 Oct 2018; revised 11 Dec 2018; accepted 11 Dec 2018; published 20 Dec 2018

Optics EXPRESS

Recently, *Woyessa* et al [13] reported the effect of the relativity humidity (RH) during annealing on the properties of PMMA based POFBGs. Such effect is due to the fact that water acts as plasticizer for PMMA and lowers its glass transition temperature (Tg). *Fasano* et al [23] investigated the effect of PMMA based POFBGs immersion in methanol/water solutions at room temperature, and a clear permanent wavelength blue shift was obtained after several hours although sealed conditions are required due to fast evaporation of methanol. *Pospori* et al [24] reported a novel thermal annealing methodology for tuning POFBGs to longer wavelengths based on stretching the optical fiber with 1% or 2% strain during the annealing process. This annealing employs hot water without a high accurate temperature control, and the same research group also demonstrated [25] that annealing under 55°C and 60 °C temperature water can also enhance the stress and force sensitivities of Bragg gratings in POF with different response time. This effect can be explained as molecular relaxation of the polymer when the fiber material temperature is raised above the β-transition temperature [26]. All these works [13,23–25] focus on permanent wavelength shift of uniform POFBG.

In this paper, we propose to produce permanent CFBGs by applying gradient thermal annealing to uniform POFBG which reduces the overall cost for fabricating POF CFBGs and leads to obtain flexible gratings response compared with strain tapered POF CFBG [20] or chirped phase mask fabrication techniques.

2. Polymer optical fiber Bragg grating fabrication

POFBGs were inscribed using a 248 nm KrF (Coherent Bragg Star Industrial-LN) laser system emitting 15 ns duration pulses. The fiber was an endlessly single-mode BDK-doped PMMA mPOF [27] which was fabricated in *DTU Fotonik* with the center hole doping technique. Before using the fiber, it was annealed with 55 °C hot water [25] for 10 mins. Details about the fabrication setup, POF cleaving and connection between POF and silica fiber for testing can be found in [28,29]. A uniform phase mask with 567.8 nm period was used to fabricate a 10 mm long FBG at 850 nm wavelength region. Figure 1 shows a uniform FBG reflected power spectrum after irradiation with a single pulse (15 ns of duration).

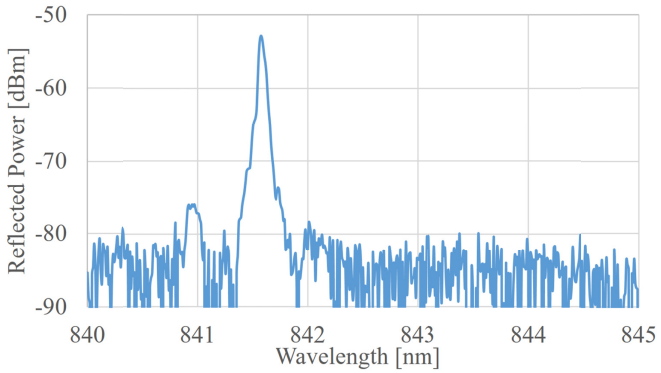

Fig. 1. Reflected spectral power of a 10 mm long uniform FBG inscribed by a single 15 ns pulse.

3. Gradient thermal annealing

The setup employed for thermal annealing is shown in Fig. 2(a) where a uniform POF grating is immersed in a container (height: 2 cm, radius 6.5 cm) filled with water (~1.4 cm height). A hot plate was used to control the temperature of the water, which was monitored by a multi-function standard CEM DT-8820 environment meter. The sensor probe was immersed in the hot water and attached to the move stage, which controls the distance from the hot plate of each measurement. The reflected spectral power of the grating was monitored by a super luminescent diode (Superlum SLD-371) and an optical spectrum analyzer (AQ6373B)

Optics EXPRESS

connected by using a silica optical fiber circulator (Thorlabs TW850R5A1). Figure 2(b) shows the temperature of the water measured at different depths of the container by moving the stage attached to the temperature sensor. As expected, the water heating by a hot plate was linear with the water depth (the temperature in the container showed a decrease of 0.23 ± 0.02 °C/mm from the bottom hot plate). In order to get uniform thermal annealing of the POFBG with a uniform temperature, the grating must be kept parallel to the hot plate, as shown in Fig. 2(a).

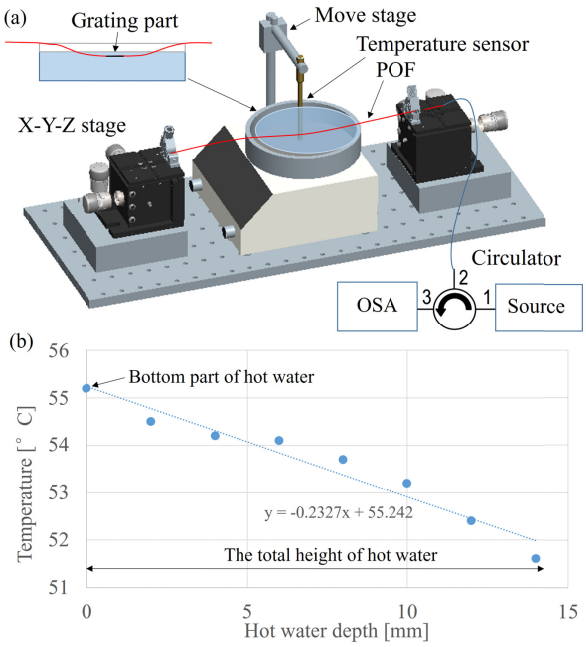

Fig. 2. (a) Experimental setup for annealing POFBG, (b) Temperature vs hot water depth in the container.

Figure 3(a) shows the Bragg wavelength shift during the annealing process with 52.5 ± 1.0 °C (grating part in ~12 mm depth of hot water). From Fig. 3(a), we can notice that the central wavelength of the grating shifts about 14 nm when the grating is brought out from the hot water after 90 mins immersion, compared to the response before immersing showing similar behavior than reported by *Pospori* et al [25] where a uniform FBG was annealed in hot water at 55 °C and 60 °C. After that, we observed that the wavelength shift was stable after 10 mins, according to stability of gratings response under humidity conditions [30]. The bandwidth of the grating evolution is also plotted in Fig. 3(a). Just after immersing in hot water, the reflected power and the bandwidth increased during the first ~4 mins, then kept considerably stable, and the reflected spectrum bandwidth remained stable during annealing (Fig. 3(b)), similar performance reported in [31]. After this process, both the wavelength and the reflected spectrum was stable after thermal annealing, as was checked after 5 days. The wavelength shift is due to the complex heterogeneous nature of fiber shrinkage and molecular relaxation [25]. *Stajanca et al* [26] also reported it under higher temperature, where the Bragg wavelength shift followed a more stretched exponential decay.

Optics EXPRESS

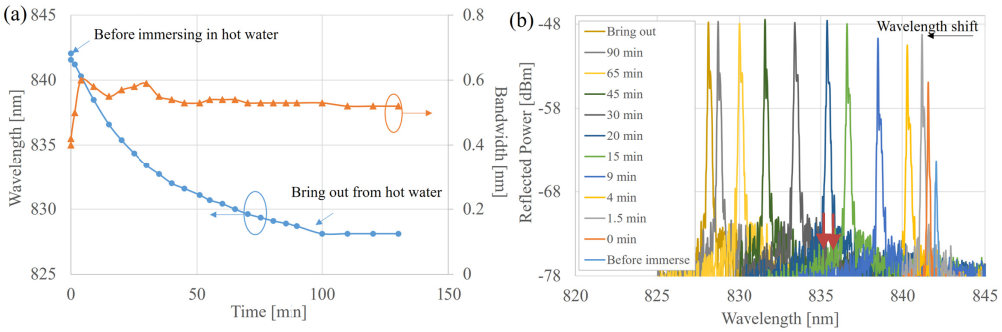

Fig. 3. Measurements during uniform annealing: (a) POFBG central wavelength and bandwidth, (b) Reflected spectral power.

Next experiment aims to use the benefits of gradient temperature in a hot water container with a hot plate at the bottom. Figure 4 shows the experimental setup for gradient thermal annealing where one magnet was used to fix the POF to the bottom of the container so the grating was immersed in the hot water at an angle of 45°, chosen to avoid damage of the fiber due to strong curvatures at steeper angles. As shown in Fig. 2(b), the linear temperature change with height in the container is 0.23 ± 0.02 °C/mm, so the temperature varies along the grating with 0.17 ± 0.02 °C/mm when the fiber was oriented at 45° angle direction.

The temperature at the bottom of the container was 55.2 ± 1 °C whereas 51.5 ± 1 °C was measured at the top (see Fig. 2(b)). Figure 5 plots the central wavelength shift with time of another FBG, similarly to Fig. 3, but showing larger wavelength shift due to higher temperature at the bottom of the container, as shown in Fig. 2(b). It is important to note that since the chirped gratings presented here and in the following have an asymmetric reflection spectrum, we define the Bragg wavelength as the center between the recorded outer edges, defined as the first minima (see marker points in Fig. 3(b)). The measurements confirm that chirped performance is obtained as Fig. 5(b) shows that the bandwidth increases from 0.3 nm to ~1.1 nm, which is more than twice the bandwidth obtained with uniform annealing in Fig. 3(a). But after ~20 minutes, although the central wavelength continued to decrease, the bandwidth stopped increasing with time.

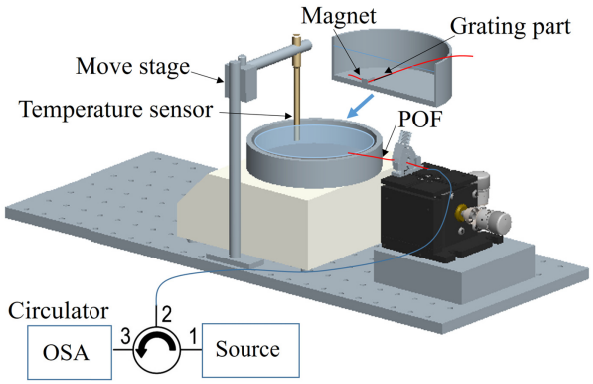

Fig. 4. Experimental setup for gradient thermal annealing.

Optics EXPRESS

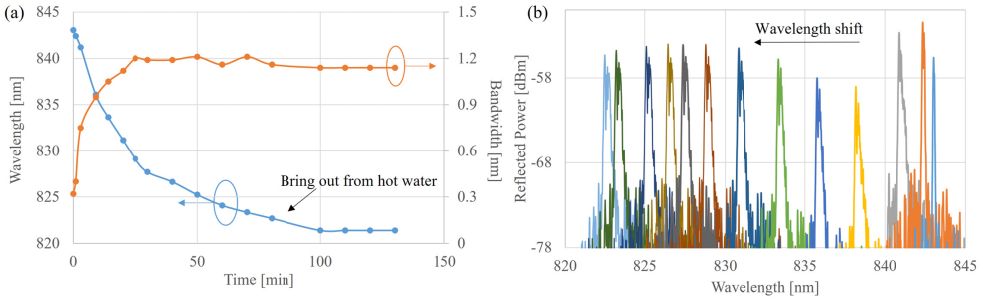

Fig. 5. Measurements during gradient annealing: (a) POFBG central wavelength shift and bandwidth, (b) Reflected spectral power.

However, the obtained chirp was somewhat limited due to the limitation in the gradient thermal annealing setup, which offered ~3 °C difference along the water container. In the following, we proposed a new method for enhanced gradient thermal annealing also based on hot water, as depicted in Fig. 6. In this case, only a 4 mm section of the POFBG was immersed in the water, whereas the rest of the grating (the total POFBG length was 10 mm) was kept outside the water. Despite the room temperature was 22 °C, the area close to the hot water container would be larger but much lower than 55 ± 1 °C, and therefore, a higher gradient thermal annealing was obtained when compared to the fully immersed grating in hot water. Figure 7 shows the obtained results with different gratings (#1, #2 and #3) under different annealing periods. Figures 7(a) and 7(c) show the spectra obtained after up to 40 s and 155 s annealing time, respectively, showing the bandwidth increases with time, with larger values than obtained in Fig. 5(a). In Fig. 7(b) and Fig. 7(d) we can observe bandwidths around 1.75 nm in ~40 s and 5.5 nm in ~150 s, which lead to group delay dispersion (GDD) values of 56.5 and 18 ps/nm, respectively, in a 1cm long grating. Once the desired chirp is achieved, the grating is brought out from hot water, although the bandwidth of the grating continued to slightly increase up to 5% as shown in Fig. 7(a). It can be considered as still having a small thermal annealing effect just after bringing it out from hot water, and then was stable afterwards. Also, the wavelength shifts 1.5 ± 0.3 nm towards the blue wavelength, as shown in Fig. 3(a), according to uniform polymer FBG response after annealing with hot water [25] whereas the bandwidth keeps roughly similar. Figures 7(e) and 7(f) show the results of another experiment (Grating 3) with longer annealing time of 510 s where the grating chirp reached 11 nm bandwidth once the grating was brought out from the water with stable behavior. Of course, the specific structure of the chirped grating, i.e. reflected spectrum, depends on the actual thermal gradient over the fiber, and therefore, fine control of the grating position relative to the water surface is required. Further work is currently being done on the time delay characterization of the chirped gratings to learn about the actual structure in order to optimize the method for obtaining chirped gratings with flat spectral response.

Optics EXPRESS

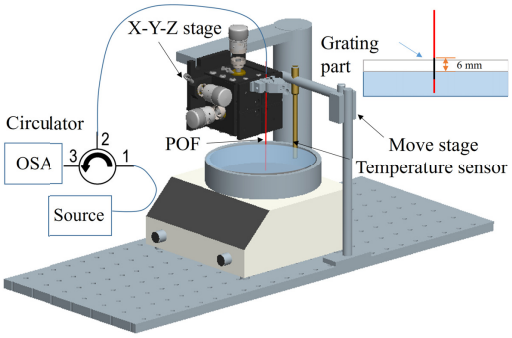

Fig. 6. Improved experimental setup for gradient thermal annealing.

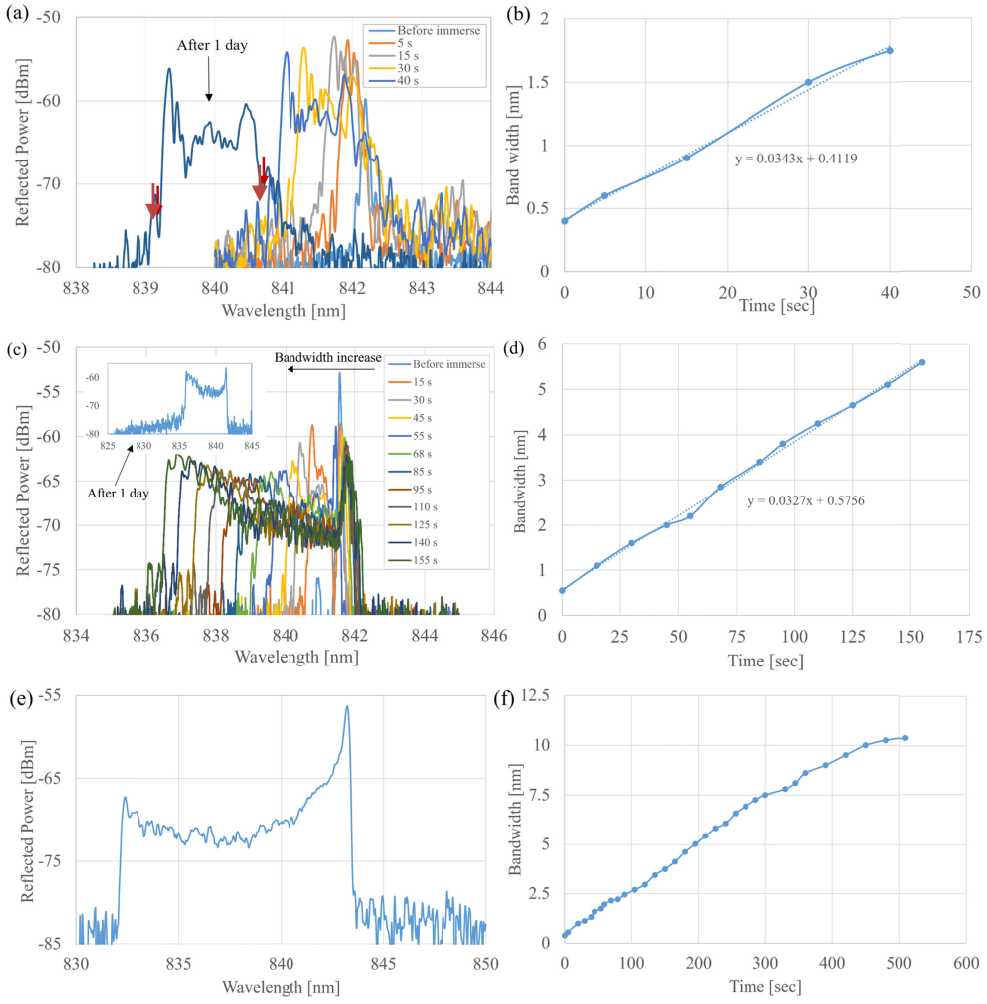

Fig. 7. POFBG under strong gradient annealing: Grating #1: (a) Reflected spectral power (total annealing time of 40 s), (b) Bandwidth vs time; Grating #2: (c) Reflected spectral power (total annealing time of 155 s), (d) Bandwidth vs time; Grating #3: (e) Reflected spectral power once the grating is brought out after 510 s annealing time, (d) Bandwidth vs time (total annealing time of 510 s).

Optics EXPRESS

4. Characterization of POF chirped FBG

In this section, we report the full characterization of the chirped POFBG obtained in Fig. 7(a) in terms of temperature, strain and humidity. The temperature sensitivity was measured by placing the grating on a Peltier plate, which contains a small v-groove and allows the temperature control by an electronic temperature controller. Some silicone grease was used to increase the temperature conduction. The central wavelength of the grating reflection bandpass was measured every 10 mins during 60 mins when temperature was changed from 27 °C to 52°C in steps of 5°. The central wavelength shifts towards the blue wavelengths about 3.2 nm (see Fig. 8(a)), which corresponds to a sensitivity around –0.106 ± 0.005 nm/°C, a bit higher than reported for uniform POFBGs about (–0.077 ± 0.007 nm/°C) [14] due to the different pre-annealing conditions. The reflected power of grating increased with temperature, whereas the bandwidth and the spectrum were similar as shown in Fig. 8(b), similar to the behavior shown by tapered CFBG under various temperature [20]. Although the reflected spectral power showed a non-flat profile, differently than reported in [20], note that the presence of peaks at both wavelength edges and, also, sharp slopes allow to provide precise measurements of the grating bandwidth and central wavelength as required for applications.

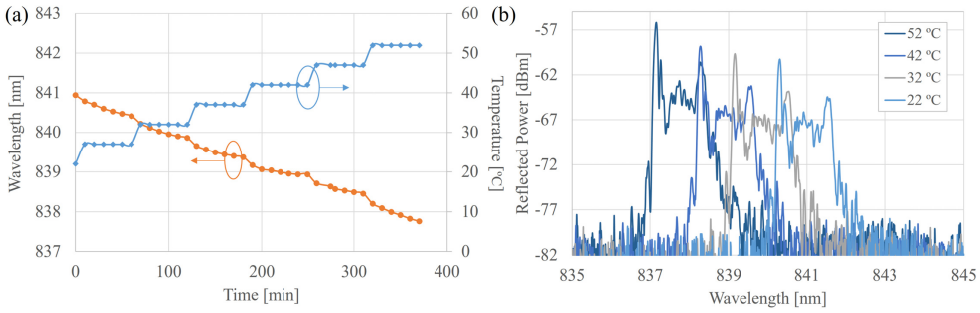

Fig. 8. (a) Central wavelength shift (the center of the wavelength spacing between the first minima (nulls)) vs time when temperature is changed. (b) Reflected spectra vs temperature.

In order to characterize the strain sensitivity of the chirped POFBG, a 15 cm long fiber containing the grating was placed on the X-Y-Z translation stage and fixed with glue between two X-Y-Z stages spaced by a distance of 11.3 cm. The fiber was strained 0.18% step-by-step awaiting 5 min between each step at room temperature. The evolution of the central wavelength was monitored when the strain was changed from 0 to 1.44% and also, decreasing it, as depicted in Fig. 9. A small hysteresis is observed in the resonance wavelength as shown in Fig. 9(a). The bandwidth keeps stable during strain, which is a different performance compared with tapered CFBG [20]. A wavelength shift of 11.6 nm was observed for the applied 1.44% strain, which indicates a linear strain sensitivity of 8.05 ± 0.05 nm/%, similarly to the results obtained with annealed PMMA mPOFBG at 850 nm spectral region [25].

Optics EXPRESS

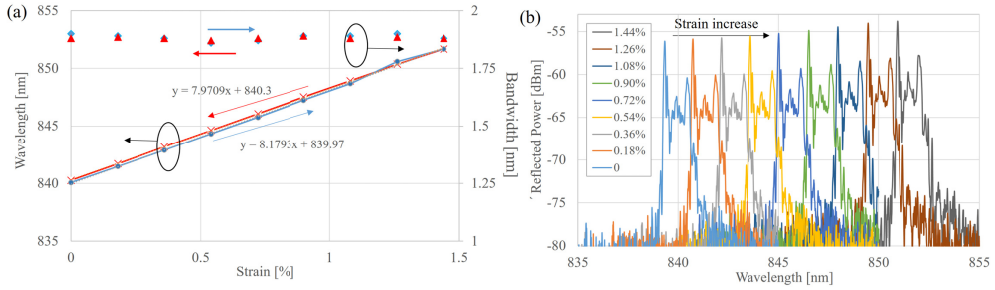

Fig. 9. (a) Central wavelength during strain increasing (blue) and decreasing (red) cycle of chirped POFBG. (b) Reflected Spectra vs strain.

Finally, the chirped POFBG was placed in the temperature chamber (Angelantoni Industrie CH340) at a constant temperature of 22 °C and 30% of relative humidity (RH) to perform the humidity characterization measurements. The RH was increased up to 90% in a step of 20% RH with a stabilization period of 70 mins. The cycle can be observed in the Fig. 10(a) and the optical spectra evolution is shown in Fig. 10(b). The total wavelength shift was 1.5 nm and the sensitivity was calculated to be 0.025 ± 0.005 nm/%RH, according to the measurements shown in Fig. 10, the obtained result is similar to one obtained with annealed phase-shifted PMMA mPOFBG at 850 nm spectral region [32].

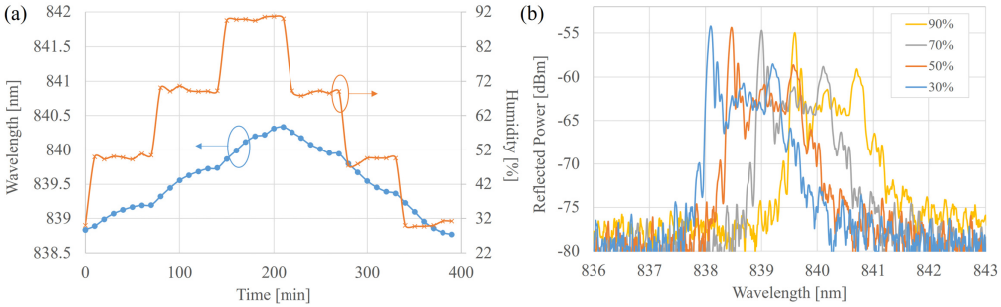

Fig. 10. (a). Central wavelength of the chirped grating vs time when humidity is changed. (b) Reflected spectrum vs humidity.

5. Conclusion

We have demonstrated a new low cost fabrication technique of chirped POFBGs based on hot water assisted gradient thermal annealing of uniform POFBGs. The proposed method is simple since no special phase mask or additional etching process is needed, and it enables an easy and flexible tuning of the wavelength and chirp performance with a permanent and stable chirp characteristic. A chirp larger than 11 nm has been obtained for the first time in less than 10 min. The central wavelength linearly changes with temperature, strain and humidity whereas the bandwidth keeps stable, similar to CFBG response when a chirped phase mask is employed for fabrication. Sensitivity measurements to external parameters have been provided for future potential applications such as high resolution large bandwidth thermal detection in bio-sensing and delay lines in microwave photonics subsystems. Moreover, the use of liquids with different specific heat coefficients will also lead to variations on the temperature gradient. In this way, investigations of different liquids and temperature gradients will be considered as future work.

Funding

Fundação para a Ciência e a Tecnologia; GVA PROMETEO; Natural Science Foundation of Heilongjiang Province.

Optics EXPRESS

Acknowledgements

This work was supported by Fundação para a Ciência e Tecnologia (FCT)/MEC through national funds, when applicable co-funded by FEDER – PT2020 partnership agreement under the project UID/EEA/50008/2013 and the Research Excellence Award Programme GVA PROMETEO 2017/103 Future Microwave Photonics Technologies and applications, Science Foundation of Heilongjiang Province of China (F2018026). C. A. F. Marques also acknowledges the financial support from FCT through the fellowship SFRH/BPD/109458/2015.

References

1. D. J. Webb, Polymer fiber Bragg grating sensors and their applications in *Optical Fiber Sensors Advanced Techniques and Applications*, G. Rajan Ed. Boca Raton, FL, USA: CRC, 257–276 (2015).
2. J. Bonefacino, H. Y. Tam, T. S. Glen, X. Cheng, C. F. J. Pun, J. Wang, P. H. Lee, M. L. V. Tse, and S. T. Boles, "Ultra-fast polymer optical fibre Bragg grating inscription for medical devices," Light Sci. Appl. **7**(3), 17161 (2018).
3. X. Cheng, J. Bonefacino, B. O. Guan, and H. Y. Tam, "All-polymer fiber-optic pH sensor," Opt. Express **26**(11), 14610–14616 (2018).
4. G. Emiliyanov, J. B. Jensen, O. Bang, P. E. Hoiby, L. H. Pedersen, E. M. Kjaer, and L. Lindvold, "Localized biosensing with Topas microstructured polymer optical fiber," Opt. Lett. **32**(5), 460–462 (2007).
5. H. U. Hassan, J. Janting, S. Aasmul, and O. Bang, "Polymer Optical Fiber Compound Parabolic Concentrator fiber tip based glucose sensor: in-Vitro Testing," IEEE Sens. J. **16**(23), 1 (2016).
6. Z. Xiong, G. D. Peng, B. Wu, and P. L. Chu, "Highly tunable Bragg gratings in single-mode polymer optical fibers," IEEE Photonics Technol. Lett. **11**(3), 352–354 (1999).
7. A. Lacraz, M. Polis, A. Theodosiou, C. Koutsides, and K. Kalli, "Femtosecond laser inscribed Bragg gratings in low loss CYTOP polymer optical fiber," IEEE Photonics Technol. Lett. **27**(7), 693–696 (2015).
8. G. Woyessa, A. Fasano, C. Markos, A. Stefani, H. K. Rasmussen, and O. Bang, "Zeonex microstructured polymer optical fiber: fabrication friendly fibers for high temperature and humidity insensitive Bragg grating sensing," Opt. Mater. Express **7**(1), 286–295 (2017).
9. A. Fasano, G. Woyessa, P. Stajanca, C. Markos, A. Stefani, K. Nielsen, H. K. Rasmussen, K. Krebber, and O. Bang, "Fabrication and characterization of polycarbonate microstructured polymer optical fibers for high-temperature-resistant fiber Bragg grating strain sensors," Opt. Mater. Express **6**(2), 649–659 (2016).
10. C. Markos, A. Stefani, K. Nielsen, H. K. Rasmussen, W. Yuan, and O. Bang, "High-Tg TOPAS microstructured polymer optical fiber for fiber Bragg grating strain sensing at 110 degrees," Opt. Express **21**(4), 4758–4765 (2013).
11. G. Woyessa, A. Fasano, A. Stefani, C. Markos, K. Nielsen, H. K. Rasmussen, and O. Bang, "Single mode step-index polymer optical fiber for humidity insensitive high temperature fiber Bragg grating sensors," Opt. Express **24**(2), 1253–1260 (2016).
12. I. P. Johnson, D. J. Webb, K. Kalli, M. C. J. Large, and A. Argyros, "Multiplexed FBG sensor recorded in multimode microstructured polymer optical fibre," Proc. SPIE **7714**, 77140 (2010).
13. G. Woyessa, K. Nielsen, A. Stefani, C. Markos, and O. Bang, "Temperature insensitive hysteresis free highly sensitive polymer optical fiber Bragg grating humidity sensor," Opt. Express **24**(2), 1206–1213 (2016).
14. W. Yuan, A. Stefani, and O. Bang, "Tunable polymer Fiber Bragg Grating (FBG) inscription: Fabrication of dual-FBG temperature compensated polymer optical fiber strain sensors," IEEE Photonics Technol. Lett. **24**(5), 401–403 (2012).
15. P. I. Reyes, N. Litchinitser, M. Sumetsky, and P. S. Westbrook, "160-Gb/s tunable dispersion slope compensator using a chirped fiber Bragg grating and a quadratic heater," IEEE Photonics Technol. Lett. **17**(4), 831–833 (2005).
16. D. Tosi, E. G. Macchi, M. Gallati, G. Braschi, A. Cigada, S. Rossi, G. Leen, and E. Lewis, "Fiber-optic chirped FBG for distributed thermal monitoring of ex-vivo radiofrequency ablation of liver," Biomed. Opt. Express **5**(6), 1799–1811 (2014).
17. D. Shan, C. Zhang, S. Kalaba, N. Mehta, G. B. Kim, Z. Liu, and J. Yang, "Flexible biodegradable citrate-based polymeric step-index optical fiber," Biomaterials **143**, 142–148 (2017).
18. H. Liu, H. Liu, G. Peng, and T. W. Whitbread, "Tunable dispersion using linearly chirped polymer optical fiber Bragg gratings with fixed center wavelength," IEEE Photonics Technol. Lett. **17**(2), 411–413 (2005).
19. C. A. F. Marques, P. Antunes, P. Mergo, D. J. Webb, and P. André, "Chirped Bragg gratings in PMMA step-index polymer optical fiber," IEEE Photonics Technol. Lett. **29**(6), 500–503 (2017).
20. R. Min, B. Ortega, and C. Marques, "Fabrication of tunable chirped mPOF Bragg gratings using a uniform phase mask," Opt. Express **26**(4), 4411–4420 (2018).
21. S. Korganbayev, R. Min, M. Jelbuldina, X. Hu, C. Caucheteur, O. Bang, B. Ortega, C. Marques, and D. Tosi, "Thermal profile detection through high-sensitivity fiber optic chirped Bragg grating on microstructured PMMA fiber," J. Lightwave Technol. **36**(20), 4723–4729 (2018).

Optics EXPRESS

22. R. Min, S. Korganbayev, C. Molardi, C. Broadway, X. Hu, C. Caucheteur, O. Bang, P. Antunes, D. Tosi, C. Marques, and B. Ortega, "Largely tunable dispersion chirped polymer FBG," Opt. Lett. **43**(20), 5106–5109 (2018).
23. A. Fasano, G. Woyessa, J. Janting, H. K. Rasmussen, and O. Bang, "Solution-mediated annealing of polymer optical fiber Bragg gratings at room temperature," IEEE Photonics Technol. Lett. **29**(8), 687–690 (2017).
24. A. Pospori, C. A. F. Marques, G. Sagias, H. Lamela-Rivera, and D. J. Webb, "Novel thermal annealing methodology for permanent tuning polymer optical fiber Bragg gratings to longer wavelengths," Opt. Express **26**(2), 1411–1421 (2018).
25. A. Pospori, C. A. F. Marques, D. Sáez-Rodríguez, K. Nielsen, O. Bang, and D. J. Webb, "Thermal and chemical treatment of polymer optical fiber Bragg grating sensors for enhanced mechanical sensitivity," Opt. Fiber Technol. **36**, 68–74 (2017).
26. P. Stajanca, O. Cetinkaya, M. Schukar, P. Mergo, D. J. Webb, and K. Krebber, "Molecular alignment relaxation in polymer optical fibers for sensing applications," Opt. Fiber Technol. **28**, 11–17 (2016).
27. X. Hu, G. Woyessa, D. Kinet, J. Janting, K. Nielsen, O. Bang, and C. Caucheteur, "BDK-doped core microstructured PMMA optical fiber for effective Bragg grating photo-inscription," Opt. Lett. **42**(11), 2209–2212 (2017).
28. A. Pospori, C. A. F. Marques, O. Bang, D. J. Webb, and P. André, "Polymer optical fiber Bragg grating inscription with a single UV laser pulse," Opt. Express **25**(8), 9028–9038 (2017).
29. D. Sáez-Rodríguez, R. Min, B. Ortega, K. Nielsen, and D. J. Webb, "Passive and Portable Polymer Optical Fiber Cleaver," IEEE Photonics Technol. Lett. **28**(24), 2834–2837 (2016).
30. W. Zhang, D. J. Webb, and G. D. Peng, "Investigation into time response of polymer fiber Bragg grating based humidity sensors," J. Lightwave Technol. **30**(8), 1090–1096 (2012).
31. A. G. Leal-Junior, A. Theodosiou, C. Marques, M. J. Pontes, K. Kalli, and A. Frizera, "Compensation Method for Temperature Cross-Sensitivity in Transverse Force Applications With FBG Sensors in POFs," J. Lightwave Technol. **36**(17), 3660–3665 (2018).
32. L. Pereira, A. Pospori, P. Antunes, M. F. Domingues, S. Marques, O. Bang, D. J. Webb, and C. Marques, "Phase-Shifted Bragg Grating Inscription in PMMA Microstructured POF Using 248-nm UV Radiation," J. Lightwave Technol. **35**(23), 5176–5184 (2017).